

Crosspolar Optimization in Reflectarray Antennas for DBS missions

Daniel R. Prado*, Manuel Arrebola†, Marcos R. Pino† and George Goussetis*

*Institute of Sensors, Signals and Systems, Heriot-Watt University, Edinburgh, U.K. Email: {dr38, g.goussetis}@hw.ac.uk

†Group of Signal Theory and Communications, Universidad de Oviedo, Spain. Email: {arrebola, mpino}@uniovi.es

Abstract—Current satellite applications for communications specify very tight cross-polarization values, usually with parameters such as the crosspolar discrimination (XPD) larger than 33 dB. To obtain these values, optimization of the cross-polarization performance has to be performed. The most common approach is to minimize the crosspolar component of the radiation pattern with regard to the copolar pattern in a subset of the visible region, corresponding to the coverage area. Nevertheless, this type of optimization provides suboptimal results since the figure of merit for cross-polarization performance (e.g. the XPD) is only optimized indirectly. Thus, in this work we propose to directly optimize the figure of merit to considerably improve the polarization purity of reflectarrays for satellite missions. For that purpose, the generalized intersection approach algorithm is employed in a very large reflectarray for a shaped beam application with European footprint. We show that directly optimizing the cross-polarization figure of merit provides better results than the usual approach of minimizing the crosspolar far field.

Index Terms—Reflectarray antennas, satellite missions, polarization purity, crosspolar discrimination (XDP), crosspolar isolation (XPI), cross-polarization performance, shaped beams

I. INTRODUCTION

The improvement of cross-polarization performance in shaped-beam reflectarray antennas for space applications is a challenging task. Some missions, such as direct broadcast satellite (DBS), require values of the crosspolar discrimination (XPD) or crosspolar isolation (XPI) parameters higher than 33 dB. Thus, some techniques are required to improve these figures of merit. The first approach for cross-polarization improvement relied in a symmetric arrangement of the reflectarray elements [1], such that contributions to the crosspolar pattern from different elements are cancelled. However, this technique presents limitations when applied to shaped-beam antennas. Another approach is to minimize, through optimization, the cross-polarization introduced by each reflectarray element [2]. In this way, the undesired tangential field at the reflectarray surface is reduced. Nevertheless, since the optimization is performed at the unit cell level, the crosspolar pattern is minimized indirectly, providing sub-optimal results.

This work was supported in part by the Ministerio de Ciencia, Innovación y Universidades under project TEC2017-86619-R (ARTEINE); by the Ministerio de Economía, Industria y Competitividad under project TEC2016-75103-C2-1-R (MYRADA); by the Gobierno del Principado de Asturias/FEDER under Project GRUPIN-IDI/2018/000191; by the Gobierno del Principado de Asturias through Programa “Clarín” de Ayudas Postdoctorales / Marie Curie-Cofund under project ACA17-09; by Ministerio de Educación, Cultura y Deporte / Programa de Movilidad “Salvador de Madariaga” (Ref. PRX18/00424).

A better approach is to directly minimize the crosspolar far field component by a direct optimization of the reflectarray layout. This was implemented for the first time in [3] using the generalized intersection approach and a full-wave analysis technique based on local periodicity (FW-LP) to analyse the reflectarray elements. However, the technique was slow, it was only able to optimize small reflectarrays and it worked with a single polarization. A number of computational improvements were introduced in [4], allowing to optimize dual-polarized reflectarrays and handling thousands of degrees of freedom. A faster approach was presented in [5], accelerating computations by using databases instead of a FW-LP tool. In all these techniques, the cost function minimizes the crosspolar component of the far field, so that the XPD and XPI parameters are improved indirectly, providing again sub-optimal results for cross-polarization performance.

In this work, it is proposed to directly optimize the XPD or XPI parameters in the cost function. In this way, the cross-polarization performance of the final reflectarray antenna will improve. It will be shown how this strategy provides better results than to directly minimize the crosspolar pattern at central frequency. For this task, the generalized intersection approach algorithm is chosen to optimize a large reflectarray for DBS service as an example of application. The optimized reflectarray is then analysed in a 5% relative bandwidth to show its performance with regard to the initial, non-optimized layout. The presented technique is general and can be employed in other applications such as synthetic radar aperture or multibeam, where cross-polarization performance is also important.

II. ANTENNA DESIGN

A. Antenna Specifications

A representation of the antenna geometry under consideration is shown in Fig. 1. The reflectarray is elliptical with a total of 4068 elements distributed in a regular grid with 74 and 70 unit cells in the main axes. The periodicity is $14\text{ mm} \times 14\text{ mm}$ while the working frequency is 11.85 GHz. The feed is modelled with a $\cos^q \theta$ function with $q = 23$, generating an illumination taper of -17.9 dB at the edges. In addition, the feed is at $(-358, 0, 1070)\text{ mm}$ with regard to the reflectarray center. The antenna is placed on a satellite in geostationary orbit at 10° E longitude. For the unit cell substrate, the bottom layer has a height of $h_A = 2.363\text{ mm}$ and a complex relative permittivity $\epsilon_{r,A} = 2.55 - j0.0023$,

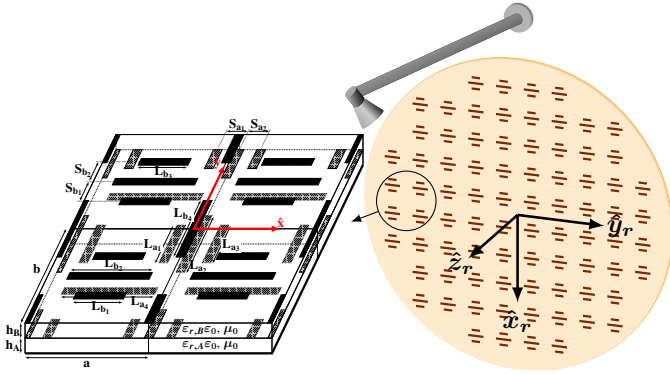


Fig. 1. Diagram of the single-offset reflectarray set-up considered in this work and the used reflectarray element for dual-linear polarization applications.

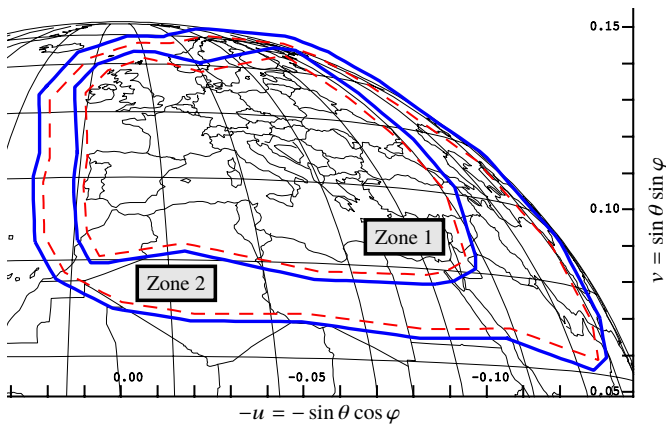


Fig. 2. European footprint with two coverage zones. The copolar requirements are 28.5 dBi and 25.2 dBi for Zones 1 and 2, respectively, and both linear polarizations [6] (© 2006 IEEE).

while the top layer has a height of $h_B = 1.524$ mm and a complex relative permittivity $\epsilon_{r,B} = 2.17 - j0.0020$.

The copolar requirements for both linear polarizations are shown in Fig. 2 and are taken from [6]. A European footprint with two distinct coverage zones has been chosen, each with a different copolar gain specifications: 28.5 dBi for Zone 1 and 25.5 dBi for Zone 2. The outer solid contours for each zone (thicker blue lines) represent the specifications taking into account typical satellite pointing errors (0.1° in roll and pitch, 0.5° in yaw). The outer contours will be employed in the optimization as well as for the representation of the obtained results.

B. The Generalized Intersection Approach

For this work, the generalized intersection approach (IA) [7] has been chosen as optimization algorithm. It is an iterative algorithm that performs two operations on the radiated field at each iteration:

$$\vec{E}_{i+1} = \mathcal{B} \left[\mathcal{F} \left(\vec{E}_i \right) \right], \quad (1)$$

where \mathcal{F} is the forward projector, which computes the radiated field and then trims it according to some specifications given

in the form of lower and upper masks; and \mathcal{B} is the backward projector, which minimizes the distance between the current radiated field by the reflectarray and the field trimmed by the forward projector that complies with the specifications [4]. A thorough mathematical description of both projectors can be consulted in [4].

The forward projector imposes the requirements of the far field by means of masks for the copolar and crosspolar patterns. In this way, following the notation in [4], the radiation pattern for both linear polarizations should fulfil the following conditions:

$$T_{cp,\min}(u, v) \leq G_{cp}(u, v) \leq T_{cp,\max}(u, v), \quad (2a)$$

$$T_{xp,\min}(u, v) \leq G_{xp}(u, v) \leq T_{xp,\max}(u, v), \quad (2b)$$

where T_{\min} and T_{\max} denote the minimum and maximum mask specifications, respectively; and G_{cp} and G_{xp} are the copolar and crosspolar components of the radiation pattern in gain, respectively. Using the conditions in (2), the crosspolar pattern is minimized and thus the XPD and XPI are optimized indirectly. Thus, in this work it is proposed to substitute the condition (2b) by another condition which takes into account the figure of merit of interest for cross-polarization performance, either the XPD or the XPI, while the condition in (2a) is left untouched to guarantee that copolar requirements are also met.

C. Initial Copolar Design

Before performing the optimization of the cross-polarization parameters, a phase-only synthesis (POS) in dual-linear polarization is carried out in order to obtain a suitable starting point for the crosspolar optimization. Thus, the followed approach is a two-step procedure. The POS produces a phase-shift that each reflectarray element must provide in order to radiate the desired copolar pattern. Then, the layout is obtained using a zero-finding routine [8], adjusting the lengths of the dipoles shown in Fig. 1. Fig. 3 shows the initial radiation pattern for polarization X simulated with a method of moments based on local periodicity (MoM-LP) [9]. As it can be seen, the copolar pattern perfectly complies with the requirements in the two coverage zones. Similar results were obtained for polarization Y. Regarding the cross-polarization performance for Zone 1, the XPD_{\min} is 31.46 dB and the XPI is 30.13 dB, the same for both linear polarizations. For Zone 2, the XPD_{\min} is 27.98 dB and 28.45 dB for polarizations X and Y, respectively; while the XPI is 25.92 dB and 26.44 dB for polarizations X and Y, respectively.

III. CROSS-POLARIZATION IMPROVEMENT

A. Optimization of XPD and XPI

For the purpose of the cross-polarization performance optimization, the XPD and XPI are considered in linear scale. Thus, the XPD is defined as the ratio, point by point, of the copolar gain and the crosspolar gain:

$$XPD(u, v) = \frac{G_{cp}(u, v)}{G_{xp}(u, v)}, \quad \forall (u, v) \in \Omega, \quad (3)$$

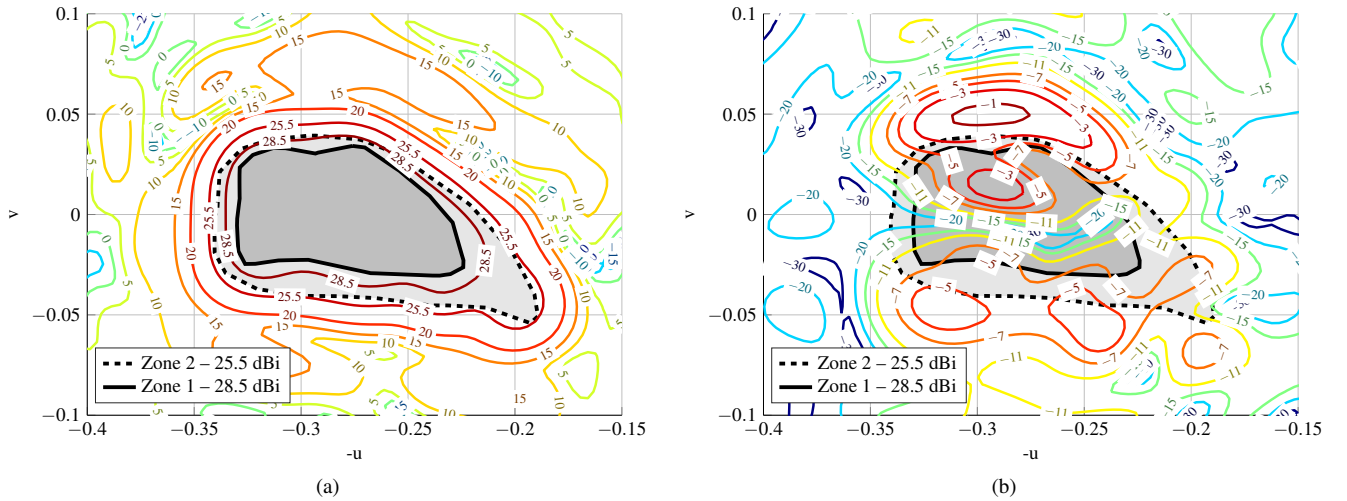


Fig. 3. Radiation pattern in dBi for polarization X obtained after the POS. (a) Copolar. (b) Crosspolar.

where Ω is a subset of the visible region ($u^2 + v^2 < 1$) corresponding to a coverage zone. The performance of the XPD is limited by its minimum value, which will be the one considered in the optimization:

$$\text{XPD}_{\min} = \min \{ \text{XPD}(u, v) \}. \quad (4)$$

Similarly, the XPI is defined as the ratio between the minimum copolar gain and the maximum crosspolar gain for each coverage zone:

$$\text{XPI} = \frac{\min \{ G_{\text{cp}}(u, v) \}}{\max \{ G_{\text{xp}}(u, v) \}}, \quad (u, v) \in \Omega. \quad (5)$$

Taking into account the definition of XPD_{\min} and XPI, the goal of the optimization is to maximize their values while maintaining the copolar pattern within specifications. Thus, only minimum mask specifications are necessary, fulfilling the following conditions:

$$T_{\text{XPD}_{\min}, \min} \leq \text{XPD}_{\min}, \quad (6a)$$

$$T_{\text{XPI}, \min} \leq \text{XPI}. \quad (6b)$$

Thus, condition (2b) in the forward projector is substituted by either (6a) or (6b), depending on the parameter that will be optimized.

B. Crosspolar Optimization Results

The proposed approach will be tested by comparing three different optimizations. The first optimization (case 1) consists in minimizing the crosspolar pattern using the condition (2b) in the forward projector. In this case, the maximum template is set 40 dB below the maximum copolar gain to reduce the crosspolar pattern as much as possible, while the minimum template is set to -200 dB. The second optimization (case 2) uses (6a) to maximize the XPD_{\min} , and the template is also set to 40 dB. Finally, the third optimization (case 3) employs the condition (6b), setting the template to 40 dB to directly improve the XPI. For all these optimizations, the starting point is the same (shown in Fig. 3), and the copolar template

specified by means of (2a) is also considered, in order to maintain the copolar gain within specifications while the crosspolarization performance is improved.

TABLE I summarizes the results for the three optimizations including the starting point as reference. In all cases, the minimum copolar gain in both coverage zones for both linear polarizations complies with the requirements of 28.5 dB for Zone 1 and 25.5 dB for Zone 2, although with slightly lower values than the starting point. Nevertheless, the crosspolarization performance was greatly improved. The first optimization strategy (case 1, i.e. minimization of the crosspolar far field) improves the XPD_{\min} and XPI between 3.18 dB and 5.19 dB. The largest improvement is for the XPI in Zone 2, since the starting point presented a very low XPI. In this case, the XPI is improved 5.19 dB in polarization X and 4.63 dB in polarization Y.

When directly optimizing the XPD_{\min} (case 2), the achieved results are considerably better. In this case, the improvement in XPD_{\min} and XPI for both coverage zones and polarizations range between 7.33 dB and 8.31 dB, which contrasts with the previous case where the improvements were lower. Since the XPD_{\min} is the optimization parameter, its improvement is better than the XPI, as shown in TABLE I. In addition, due to the definitions in (4) and (5), the XPI is a stricter parameter than the XPD_{\min} , and the XPI will be always lower or equal than the XPD_{\min} , regardless of the parameter which is object of the optimization. Finally, optimizing the XPI (case 3) improves the results of the XPI parameter with regard to the previous case, while keeping the overall improvement of the cross-polarization performance higher than when minimizing the crosspolar pattern.

Tables II and III summarize the improvement in crosspolarization performance for the three strategies with regard to the starting point. The new proposed approach to directly improve the XPD_{\min} (case 2) or XPI (case 3) provides results that are 3 dB to 5 dB better than when minimizing the crosspolar pattern (case 1). Meanwhile, Fig. 4 shows the

TABLE I

RESULTS OF THE DIRECT OPTIMIZATION OF A REFLECTARRAY WITH A EUROPEAN FOOTPRINT WITH TWO COVERAGE ZONES COMPARING DIFFERENT STRATEGIES: THE USUAL APPROACH OF MINIMIZING THE CROSSPOLAR COMPONENT OF THE RADIATION PATTERN (CASE 1) AND THE NEW STRATEGY OF DIRECTLY OPTIMIZING THE FIGURE OF MERIT (CASE 2 FOR XPD_{\min} OPT. AND CASE 3 FOR XPI OPT.) CP_{\min} IS IN DBI, XPD_{\min} AND XPI ARE IN DB.

	Zone 1 (28.5 dBi)						Zone 2 (25.5 dBi)					
	Pol. X			Pol. Y			Pol. X			Pol. Y		
	CP_{\min}	XPD_{\min}	XPI	CP_{\min}	XPD_{\min}	XPI	CP_{\min}	XPD_{\min}	XPI	CP_{\min}	XPD_{\min}	XPI
Initial	29.29	31.46	30.13	29.32	31.46	30.13	26.03	27.98	25.92	26.03	28.45	26.44
Case 1	29.30	35.10	34.57	29.26	35.60	33.38	26.27	31.85	31.11	26.31	31.63	31.07
Case 2	29.00	39.64	37.46	29.08	39.36	37.46	25.96	35.96	33.46	25.67	36.76	33.81
Case 3	29.04	39.53	39.25	29.01	40.32	39.00	25.80	34.78	34.49	26.06	36.29	35.75

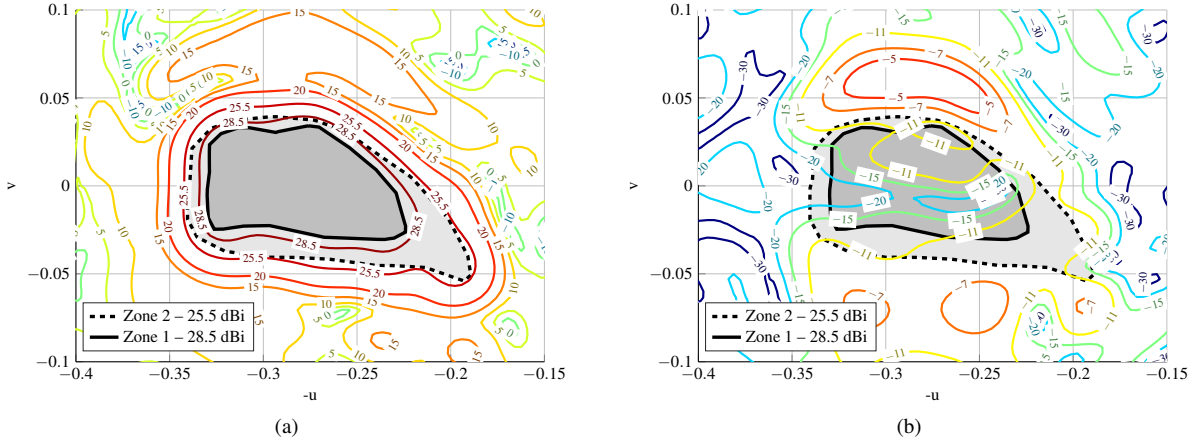


Fig. 4. Obtained radiation pattern in dBi for polarization X after the XPD_{\min} optimization (case 2). (a) Copolar. (b) Crosspolar.

TABLE II
CROSS-POLARIZATION PERFORMANCE IMPROVEMENT (DB) FOR ZONE 1.

	Pol. X		Pol. Y	
	XPD_{\min}	XPI	XPD_{\min}	XPI
Case 1	3.64	4.44	4.14	3.25
Case 2	8.18	7.33	7.90	7.33
Case 3	8.07	9.12	8.86	8.87

TABLE III
CROSS-POLARIZATION PERFORMANCE IMPROVEMENT (DB) FOR ZONE 2.

	Pol. X		Pol. Y	
	XPD_{\min}	XPI	XPD_{\min}	XPI
Case 1	3.87	5.19	3.18	4.63
Case 2	7.98	7.54	8.31	7.37
Case 3	6.80	8.57	7.84	9.31

optimized radiation pattern for polarization X for the XPD_{\min} optimization. Compared with Fig. 3, it can be seen how the copolar gain is barely affected, while the crosspolar pattern is significantly reduced, specially in the two coverage areas.

Finally, the optimized reflectarray for case 2 (direct optimization of the XPD_{\min} parameter), was simulated in a 5% bandwidth and compared with the initial design. The extreme frequencies are 11.55 GHz and 12.15 GHz, for which the q value of the feed model was set to 21.7 and 26.3, respectively, to simulate the variation of the feed directivity with frequency. TABLE IV shows the results for the initial layout before the optimization and the optimization for case 2. As it can be seen, the cross-polarization performance of the optimized layout at central frequency is still better than the initial layout, although due to the narrow bandwidth nature of reflectarray antennas [8], the copolar pattern does not comply with specifications. Nevertheless, the drop in minimum copolar gain in the considered bandwidth is small. In fact, in most cases, a compliance better than 90% is achieved in both coverage zones, with the worst case produced for zone 1 at 12.15 GHz for polarization Y, with a compliance for copolar gain of 84.7% in the whole zone. Fig. 5 shows the radiation patterns at extreme frequencies for polarization X. The copolar pattern shape is slightly deteriorated, and the drop in minimum copolar gain value occurs at a few points, hence keeping a compliance better than 95% for this polarization. Nevertheless, this bandwidth analysis demonstrates the need for a multifrequency design procedure in reflectarray antenna to achieve broadband performance.

TABLE IV
COMPARISON OF THE PERFORMANCE OF THE INITIAL REFLECTARRAY LAYOUT AND THE OPTIMIZED LAYOUT FOR CASE 2 (XPD_{\min} OPTIMIZATION) IN A 5% RELATIVE BANDWIDTH AT EXTREME FREQUENCIES (11.55 GHz AND 12.15 GHz).

	Zone 1 (28.5 dBi)						Zone 2 (25.5 dBi)					
	Pol. X			Pol. Y			Pol. X			Pol. Y		
	CP_{\min}	XPD_{\min}	XPI	CP_{\min}	XPD_{\min}	XPI	CP_{\min}	XPD_{\min}	XPI	CP_{\min}	XPD_{\min}	XPI
11.55 GHz (initial)	28.56	30.57	29.16	28.24	31.03	28.81	24.98	30.57	25.59	24.98	28.24	25.55
12.15 GHz (initial)	28.43	33.00	32.05	28.03	32.43	31.91	25.09	30.49	28.05	26.36	31.32	29.03
11.55 GHz (case 2)	28.28	37.06	35.04	27.85	33.02	30.52	24.74	34.10	31.50	24.63	30.79	27.30
12.15 GHz (case 2)	28.46	34.20	33.07	28.04	34.35	33.30	25.03	31.30	29.65	25.87	33.75	33.75

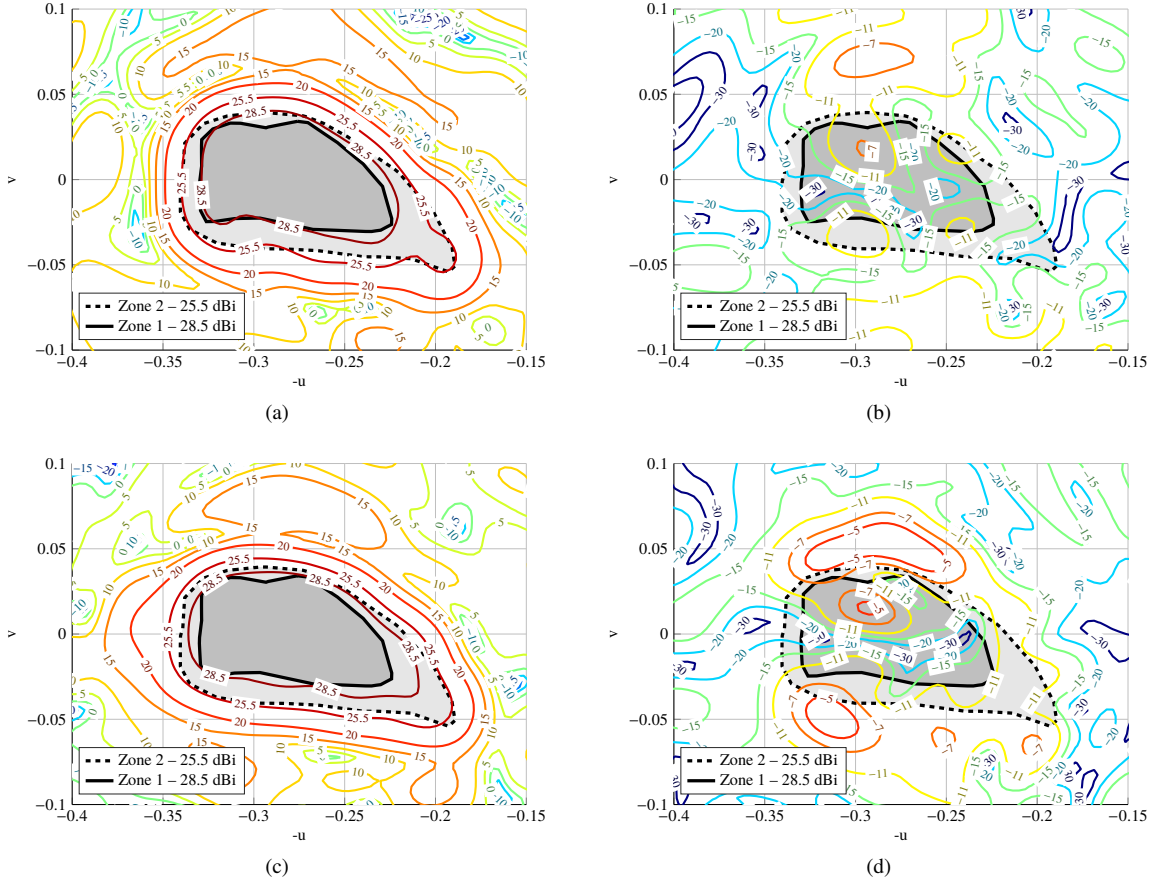


Fig. 5. Simulated radiation patterns in a 5% relative bandwidth of the optimized layout for case 2 (XPD_{\min} optimization) for polarization X. (a) Copolar pattern at 11.55 GHz. (b) Crosspolar pattern at 11.55 GHz. (c) Copolar pattern at 12.15 GHz. (d) Crosspolar pattern at 12.15 GHz.

IV. CONCLUSION

This work has proposed the direct optimization of the figure of merit for cross-polarization to improve the performance of the final antenna. The usual approach consists in the minimization of the crosspolar component of the far field, so parameters such as the crosspolar discrimination (XPD) or crosspolar isolation (XPI) are optimized indirectly. Thus, in this work the direct optimization of the XPD and XPI has been addressed to improve the cross-polarization performance of reflectarrays for space applications. The chosen algorithm is the generalized intersection approach, where the

copolar and crosspolar requirements are specified as minimum and maximum masks. Thus, by properly setting minimum masks attending to the definition of XPD_{\min} and XPI, those parameters can be effectively optimized. As an example, a large reflectarray for direct broadcast satellite application with a European footprint with two different coverage zones. As starting point, a layout obtained after a phase-only synthesis is employed. Then, the geometry of the reflectarray was directly optimized following three different strategies: first, minimizing the crosspolar pattern, then maximizing the XPD_{\min} and finally maximizing the XPI.

The results show that all three strategies improve the cross-polarization performance while keeping the copolar pattern within requirements. However, the new proposed approach of directly improving the XPD_{\min} or XPI provides results that are 3 dB to 5 dB better than when minimizing the crosspolar pattern. This means that the improvement over the starting point is better than 7 dB, and reaches an improvement in the XPI of more than 9 dB. The reflectarray was also simulated in a 5% relative bandwidth, and the optimized layout shows improved cross-polarization performance in that bandwidth with regard to the initial layout despite the deterioration of the copolar pattern due to the narrow bandwidth nature of reflectarray antennas. Finally, the proposed strategy may be applied to circular polarized reflectarrays as well as to the optimization over a certain bandwidth.

REFERENCES

- [1] D.-C. Chang and M.-C. Huang, "Multiple-polarization microstrip reflectarray antenna with high efficiency and low cross-polarization," *IEEE Trans. Antennas Propag.*, vol. 43, no. 8, pp. 829–834, Aug. 1995.
- [2] R. Florencio, J. A. Encinar, R. R. Boix, G. Pérez-Palomino, and G. Toso, "Cross-polar reduction in reflectarray antennas by means of element rotation," in *10th European Conference on Antennas and Propagation (EuCAP)*, Davos, Switzerland, Apr. 10–15, 2016, pp. 1–5.
- [3] O. M. Bucci, A. Capozzoli, G. D'Elia, and S. Musto, "A new approach to the power pattern synthesis of reflectarrays," in *Proc. URSI International Symposium on Electromagnetic Theory (EMTS'04)*, Pisa, Italy, May 23–27, 2004, pp. 1053–1055.
- [4] D. R. Prado, M. Arrebola, M. R. Pino, R. Florencio, R. R. Boix, J. A. Encinar, and F. Las-Heras, "Efficient crosspolar optimization of shaped-beam dual-polarized reflectarrays using full-wave analysis for the antenna element characterization," *IEEE Trans. Antennas Propag.*, vol. 65, no. 2, pp. 623–635, Feb. 2017.
- [5] M. Zhou, S. B. Sørensen, O. S. Kim, E. Jørgensen, P. Meincke, and O. Breinbjerg, "Direct optimization of printed reflectarrays for contoured beam satellite antenna applications," *IEEE Trans. Antennas Propag.*, vol. 61, no. 4, pp. 1995–2004, Apr. 2013.
- [6] J. A. Encinar, L. S. Datashvili, J. A. Zornoza, M. Arrebola, M. Sierra-Castaner, J. L. Besada-Sanmartin, H. Baier, and H. Legay, "Dual-polarization dual-coverage reflectarray for space applications," *IEEE Trans. Antennas Propag.*, vol. 54, no. 10, pp. 2827–2837, Oct. 2006.
- [7] O. M. Bucci, G. D'Elia, G. Mazzarella, and G. Panariello, "Antenna pattern synthesis: a new general approach," *Proc. IEEE*, vol. 82, no. 3, pp. 358–371, Mar. 1994.
- [8] J. Huang and J. A. Encinar, *Reflectarray Antennas*. Hoboken, NJ, USA: John Wiley & Sons, 2008.
- [9] R. Florencio, J. A. Encinar, R. R. Boix, V. Losada, and G. Toso, "Reflectarray antennas for dual polarization and broadband telecom satellite applications," *IEEE Trans. Antennas Propag.*, vol. 63, no. 4, pp. 1234–1246, Apr. 2015.